Manhole cover detection using a geometrical filter on very high resolution aerial and satellite images.

Olivier Bartoli*, Nanée Chahinian*, Aude Allard†, Jean-Stéphane Bailly‡, Katia Chancibault†, Fabrice Rodriguez†, Christian Salles§, Marie-George Tournoud§ and Carole Delenne§
* IRD, UMR HSM 5569 (CNRS, IRD, Univ. Montpellier), France
† IFSTTAR, Lab. Eau et Environnement, Nantes, France
‡ Agro'ParisTech, UMR LISAH (INRA, IRD, SupAgro), Montpellier, France
§ Univ. Montpellier, UMR HSM 5569 (CNRS, IRD, Univ. Montpellier), France

***Abstract*—One of the direct consequences of urban growth is the multiplication of buried utility networks. It is difficult to obtain complete and accurate maps of these networks because they have often been produced by different parties at different times. This work aims at putting forward a methodology to detect manhole covers on high resolution images, in order to reconstruct an urban drainage network. A circular detection filter is applied to high resolution orthophotos and Pléiade images to pinpoint mahole covers. The primary results are encouraging as 42% of manhole covers are detected by this method. Further work is carried out to improve the method and extend it to rectangular grates, that are not detected by the circular filter.**

I. Introduction

Regardless of economic growth, urban expansion is an ongoing trend [1] [2] and urban areas are viewed as particularly vulnerable to climate change; current forecasts predict increasing poverty and rapid urbanization [3]. Hence, urban areas are highly sensitive and need frequent monitoring. Remote sensing applications in urban areas have mainly focused on identifying and estimating urbanized surfaces and urban sprawl, quantifying urban microclimate and urban heart islands [4] [5] [6] [7] [8]. As the spatial resolution of the images improved, specific elements of the urban landscape could be identified [9]. Hence, nowadays images are used to detect road networks [10] [11], urban vegetation [12] and building characteristics [13] [14] [15]. They thus become part and parcel of urban management tools. There is however a domain where using high resolution imagery could be a useful tool and where currently few if any studies are available: underground utilities' management. Indeed, buried utilities are often connected to the ground surface through objects such as manhole covers and grates which can be identified on high resolution images and be used as landmarks for the geolocalization of these networks. Mispositioning of buried utilities is an increasingly important problem both in industrialized and developing countries because of urban sprawl and technological advances which create new needs among consumers resulting in additional cables and pipes that have to be added and connected [16] [17].

The main objective of this paper is to put forward a methodology to detect manhole covers and grates on high resolution orthorectified areal photographs. The methodology is tested on a small town in southern France (Gigean, Herault).

II. Materials and methods

Orthophotos of the town of Gigean (Herault, South of France) with a 25 cm resolution and Pléiades bundle products (50 cm resolution) were used to put forward the method. Ground truth was acquired on three residential zones (Zone 1 to 3 in Fig. 1). It was subsequently tested on two parking areas: one in Gigean and another in the city of Montpellier. A 16 cm resolution orthophoto obtained via the citys online portal (http://opendata.montpelliernumerique.fr/Orthophoto-2013) was used for this purpose.

The Gigean orthophotos were kindly provided by SIG-LR while the Pléiades images were obtained through the SUDOC project.

Fig. 1. Orthophoto of Gigean, south of France ©SIG-LR 2014, and location of the four testing zones used to validate the approach (see part Results).

The methodology is threefold. First the image is segmented to extract the zones where manhole covers and grates can be found *i.e.* roads, streets and pavements. Then the vegetation and shadows are eliminated by using colorimetric indices, using infrared information provided by Pléiade images. Finally

978-1-4799-6652-3/15/$31.00 © 2015 IEEE

the circular object detection method proposed in [18] is used to locate the manhole covers and grates.

A. Image segmentation

1) Roads detection: several methods were tested to extract the road. The most efficient one in terms of implementation simplicity, calculation time and final results, consists in selecting all the light grey pixels in the image, *i.e.* pixels having a low intensity in all channels of the image. The average value of each pixel over the three channels (Red, Green, Blue) is computed and the pixel is classified as "road" if its radiometric value in each channel deviates from the mean value of less than a given threshold. In this application the threshold was set to 10%.

Classified pixels are then merged into connected components using the union-find algorithm. The roads are expected to constitute large connected components; hence the smallest units (smaller 1000 pixels) are eliminated (Fig. 2).

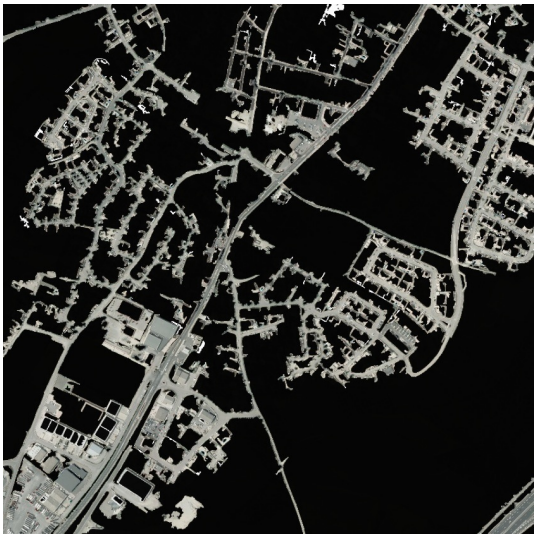

Fig. 2. Roads detection using grey-level threshold and extraction fo the biggest connected components.

2) Vegetation and shadow removal: two indices are used to segment the vegetation. The classical NDVI uses the Near InfraRed (NIR) information of the Pléiades images in contrast with the Red (R) band: NDVI = (NIR-R)/(NIR+R). The ExG index (Excess Green) is used on the areal orthophotos which do not have a NIR channel; it is defined as: ExG = 2G-R-B. The results are then combined to benefit from the spectral resolution of the Pléiades images and the spatial resolution of the orthophotos.

The shadow elimination procedure is based on Dempster-Shafer's evidence theory following a method presented in [19]. A final smoothing using the Iterated Conditional Modes (ICM) algorithm is performed (Fig. 4). The resulting shadow characteristic image is then combined to the vegetation image to clean the orthophotos from areas not supposed to contain manhole covers.

B. Cirular object detection

The geometrical approach is based on the method proposed in [18] for the detection of circular patterns in a noisy and low

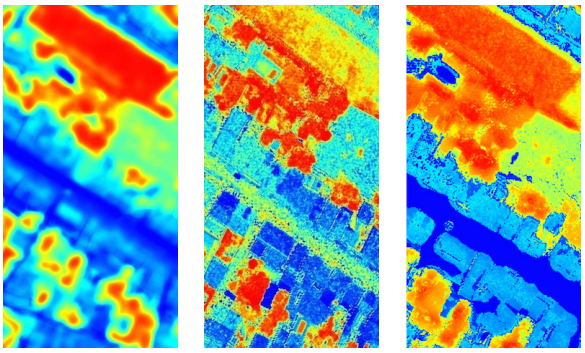

Fig. 3. Detection of vegetation using, left: NDVI, middle: ExG and right: fusion of the two previous results. The red (resp. blue) color indicates a high (resp. low) probability for the pixel to belongs to vegetation class.

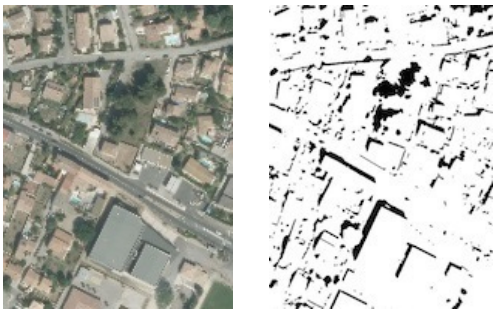

Fig. 4. Shadow elimination from [19] and applying an ICM algorithm to smooth results.

contrasted image. The authors put forward a filter that consists of two annular regions R_1 and R_2 of radius r_1 to r and r to r_2, each of which is divided in eight sub-regions (see Fig. 5). The filter is applied to a grey-scaled image, obtained with the luminance formula.

Three indices are computed to detect a circular pattern on a sliding window, using normalized histograms of each region/subregion.

The first one estimates the similarity between two statistical distributions using the Bhattacharyya coefficient:

$$\mathrm{S}(R_1, R_2) = \sum_{x=0}^{N} \sqrt{p_1(x) p_2(x)} \tag{1}$$

where p_1 (respectively p_2) is the normalized histogram of R_1 (respectively R_2) and N is the maximal intensity of the two histograms. The result of this index is 1.0 when the two histograms are identical and 0.0 when they are completely different. The desirable value for this index in case of a circular pattern is thus the lower.

The second index is computed to avoid detection of linear patterns. It is based on the comparison between the intensity distribution of R_1 and those of the eight sub-regions of R_2:

$$\mathrm{S}_8 = \max_{j \in 1 \ldots 8} \left\{ \mathrm{S}(R_1, S_2^j) \right\} \tag{2}$$

where S_2^j denotes the j^{th} subregion of R_2. This index is low when all oriented similarity scores between R_1 and R_2's subregions are small.

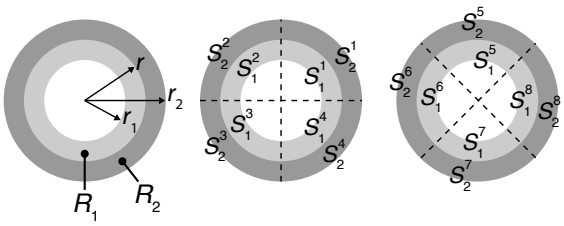

Fig. 5. Circular filter (from [18]). Left: R_1 and R_2 are the two main regions; middle and right: definition of the subregions (the phase shift is $\pi/4$).

The last index assesses the uniformity within the two main regions:

$$\mathrm{U}(R_i) = \min_{j,j' \in \{1..8\}} \left\{ \mathrm{S}(S_i^j, S_i^{j'}) \right\} \quad (3)$$

where i stands for the region and j, j' for the subregions.

The three index are finally merged in a global index for circular pattern detection:

$$\zeta = (1 - \max\{\mathrm{S}(R_1, R_2), \mathrm{S}_8\}) \cdot \mathrm{U}(R_1) \cdot \mathrm{U}(R_2) \quad (4)$$

The higher the value of ζ, the higher the probability of encountering a circular shaped object.

III. Results

The method is applied on four test zones extracted from a 5000*5000 pixel image. Three of the test zones correspond to housing estates for which a ground truth is available, while the last one is a lorry parking zone.

TABLE I. Detection results in residential areas

Zones	1	2	3
Manholes per zone (nb)	26	19	19
Detected objects (nb)	23	21	13
True positives (nb)	12	11	4
False positives (nb)	11	10	9
Detected manholes (%)	46%	58%	21%
Undetected manholes (%)	54%	42%	79%
False detection (%)	47%	47%	69%

The primary results indicate (Tab. I) that the filter is able to detect manhole covers, in all three zones with slightly better results for zone 2 and poorer results for zone3. As the three zones are residential areas with similar semi-detached houses, the difference in results is thought to be caused by a higher proportion of vegetation and shadows. Fig. 6 shows examples of true and false positives as well as undetected objects.

Fig. 6. Examples of results. Left: true positive, middle: undetected; right: false positive.

The results also highlight the existence of false positives, reaching nearly 60% in zone 3. No clear typology of the situations which lead to false detection can be made at this stage. Finally, despite our best efforts and successive filtering processes, 42% to 79% of manholes remain undetected. This may seem as a poor result, however, it is common practice in southern France not to systematically take down all manhole locations during surveying, but rather to register only half or one third of covers each time, in an effort to cut down costs.

Fig. 7. Results obtained on left: the lorry parking zone; right: HSM parking lot.

The results obtained on the lorry parking zone (Fig. 7 left) are harder to quantify because no ground truth is available to validate the detection. However, based on the location and the density of the detection patches, it can be assumed that the results are relatively poor. Patches corresponding to oil spills are confused as manhole covers. This indicates the need for additional rules to eliminate false positives.

To overcome the lack of validation, the method was tested on an orthophotoplan of our lab's parking lot located in Montpellier (image with a 16 cm ground resolution provided by the city of Montpellier). There are less oil patches on this parking lot but bigger metallic plates belonging to the telephone network can be seen. The detection results are satisfactory (Fig. 7 right): despite a higher proportion of false positives (10 over 24 detected objects) more manhole covers are detected *i.e.* 14 over a total of 22 manhole covers present on the image.

IV. Conclusion and perspectives

The purpose of this work was to detect manhole covers on high resolution images. The main challenge was to detect grey objects whose size is within the spatial resolution limit of the image and that are located on a grey background. The primary results obtained this far are satisfactory as they allow the detection of 42% of manhole covers in residential areas. Surveying companies in southern France are often required to report one third of manholes in order to cut down production costs. Our method thus allows the same detection rate.

The final objective of this project is to estimate urban contribution to downstream waterbodies and not to precisely assess water fluxes in the network itself. Based on the detected manhole covers locations, and knowing the efficiency of the method, a network will be statistically reconstructed using the rules and regulations of drainage network implementation in France. A sensitivity analysis will also be performed to estimate the impact the partial information on network characteristics have on the assessment of downstream fluxes.

Acknowledgment

This work has been suported by the Programme National de Télédétection Spatiale (PNTS, http://www.insu.cnrs.fr/actions-

sur-projets/pnts-programme-national-deteledetection-spatiale), grant n PNTS-2014-01 .

This work was supported by public funds received in the framework of GEOSUD, a project (ANR-10-EQPX-20) of the program "Investissements d'Avenir" managed by the French National Research Agency".

The orthophotos of Gigean were kindly provided by SIG-LR and those of Montpellier were obtained via the citys online portal (http://opendata.montpelliernumerique.fr/Orthophoto-2013).

REFERENCES

[1] S. Poelhekke, "Urban growth and uninsured rural risk: Booming towns in bust times," *Journal of Development Economics*, no. 96, pp. 461–475, 2011.

[2] D. Burns, V. T., J. McDonnell, J. Hasseth, J. Duncan, and C. Kendall, "Effects of suburban development on runoff generation in the croton river basin, new york, usa," *Journal of Hydrology*, no. 311, pp. 266–281, 2005.

[3] R. Gasper, A. Blohm, and M. Ruth, "Social and economic impacts of climate change on the urban environment," *Current Opinion in Environmental Sustainability*, no. 3, pp. 150–157, 2011.

[4] Q. Weng, "Remote sensing of impervious surfaces in the urban areas: Requirements, methods and trends," *Remote sensing of the environment*, no. 117, pp. 34–49, 2011.

[5] G. Xian and M. Crane, "Assessments of urban growth in the tampa bay watershed using remote sensing data," *Remote Sensing of Environment*, no. 97, pp. 203–215, 2005.

[6] S. Arthur-Hartranft, T. Carlson, and K. Clarke, "Satellite and ground-based microclimate and hydrologic analyses coupled with a regional urban growth model," *Remote sensing of the environment*, no. 86, pp. 385–400, 2003.

[7] B. Dousset and F. Gourmelon, "Satellite multi-sensor data analysis of urban surface temperatures and landcover," *ISPRS Journal of Photogrammetry and Remote Sensing*, no. 58, pp. 45–54, 2003.

[8] K. Gallo, J. Tarpley, A. McNab, and T. Karl, "Assessment of urban heat islands: a satellite perspective," *Atmospheric research*, no. 37, pp. 37–43, 1994.

[9] S. Bhaskaran, S. Paramanada, and M. Ramanayan, "Per-pixel and object-oriented classification methods for zapping urban features using ikonos satellite data," *Applied Geography*, no. 30, pp. 630–665, 2010.

[10] R. Péteri and T. Ranchin, "Potentialités des nouveaux capteurs à très haute résolution spatiale pour l'extraction des réseaux de rues urbains," *Revue Internationale de Géomatique*, no. 14, pp. 485–504, 2004.

[11] R. Stoica, X. Descombes, and J. Zerubia, "A gibbs point process for road extraction from remotely sensed images," *International Journal of Computer Vision*, no. 57, pp. 121–136, 2004.

[12] B. Höfle, M. Hollaus, and J. Hagenauer, "Urban vegetation detection using radiometrically calibrated small-footprint full-waveform airborne lidar data," *ISPRS Journal of Photogrammetry and Remote Sensing*, no. 67, pp. 134–147, 2012.

[13] T. Hermosilla, L. Ruiz, J. Recio, and J. Estornell, "Evaluation of automatic building detection approaches combining high resolution images and lidar data," *Remote Sensing*, no. 3, pp. 1188–1210, 2011.

[14] S. Freire, T. Santos, N. Gomes, A. Fonseca, and A. Tenedó, "Extraction of building from quickbird imagery for municipal use: the relevence of urban context and heterogeneity," in *R. Reuter (Editor), 30th EARSeL Symposium. Remote sensing for science, education, and natural and cultural heritage.*, EARSeL, Paris, France, 2010, pp. 131–137.

[15] S. Lhomme, C. Weber, D.-C. He, D. Morin, and A. Puissant, "Building extraction from very high spatial resolution image," in *Xth congress of the International Society for Photogrammetry and Remote Sensing*, Istanbul, Turkey, 2004, pp. 12–23.

[16] H. Jamil, N. Z., and M. Mohid Yussof, "Underground utility mapping and its challenges in malaysia," in *FIG working week 2012. Knowing to manage the territory, protect the environment, evaluate the cultural heritage*, Rome, Italy, 2012, p. 15.

[17] N. Metje, P. Atkins, M. Brennan, D. Champan, H. Lim, J. Machell, J. Muggleton, S. Pennock, J. Ratcliffe, M. Redfern, C. Rogers, A. Saul, Q. Shan, S. Swingler, and A. Thomas, "Mapping the underworld: State of the art review," *Tunnelling and underground space technology*, no. 22, pp. 568–586, 2007.

[18] H. Niigaki, J. Shimamura, and M. Morimoto, "Circular objet detection based on seperability and uniformity of feature distributions using bhattacharrya coefficient," in *21st International conference on pattern regocnition (ICPR 2012)*, Tsukuba, Japan, 2012, pp. 2009–2012.

[19] T.-T. Ngo, C. Collet, and V. Mazet, "Détection simultanée de l'ombre et la végétation sur des images aériennes couleur en haute résolution," in *RIFA*, 2014.